Laser Radar for Spacecraft Guidance Applications

Carl Christian Liebe, Alex Abramovici, Randy K. Bartman, Robert L. Bunker, Jacob Chapsky, Cheng-Chih Chu, Daniel Clouse, James W. Dillon, Bob Hausmann, Hamid Hemmati, Richard P. Kornfeld, Clint Kwa, Sohrab Mobasser, Michael Newell, Curtis Padgett, W. Thomas Roberts, Gary Spiers, Zachary Warfield, Malcolm Wright

Jet Propulsion Laboratory (JPL), California Institute of Technology
4800 Oak Grove Dr., Pasadena CA 91109-8099
818 354 7837
carl.c.liebe@jpl.nasa.gov

Abstract — A flight qualified laser radar called LAMP (LAser MaPper) is under development at JPL. LAMP is a guidance and control sensor that can form 3 dimensional images of its field of regard. The maps can be used for spacecraft rendezvous, docking, and hazard avoidance during landing and for rover traverse planning. LAMP operates by emitting high power, short duration laser pulses, which are directed by an internal gimbaled mirror in azimuth and elevation. When the laser pulses impinge on a surface, a small amount of the light is reflected back to the sensor and is collected by a telescope. On the way out, a laser actuated trigger starts a counter that is stopped by the return pulse. The counter value (time of flight) is proportional to the distance to the object. This paper describes the detailed design of the LAMP sensor.

TABLE OF CONTENTS

1. INTRODUCTION

A flight qualified, low mass, and low power 3 dimensional laser radar will enable a number of new missions and capabilities [1]. Therefore, the Mars Technology Program at JPL has undertaken the development of a laser radar for guidance and navigation applications. The development of the instrument called LAMP (LAser MaPper) was initiated in year 2000 and will be flight demonstrated in year 2004 [2].

A laser range finder is a device that measures the distance to a target, but the beam orientation is fixed. This is different from a laser radar, where the orientation of the beam can be changed. Laser range finders have been demonstrated on a number of previous missions as shown in Table 1. The primary use of laser range finders has been to obtain scientific data. This is fundamentally different from LAMP that will be used as a guidance and navigation sensor.

Table 1. Missions using laser range finders

Mission	Year	Functionality	Status
Apollo 15	1971	Ranging	Success
Mars Orbiter Laser Altimeter 1	1992	Ranging	Spacecraft lost
Clementine	1994	Ranging	Success
Lidar Inspace Technology experiment	1994	Profiling	Success
Balkan	1995	Profiling	Success
NEAR	1996	Ranging	Success
Shuttle Laser Altimeter 1	1996	Ranging	Success
Mars Orbiter Laser Altimeter 2	1996	Ranging	Success
Shuttle Laser Altimeter 2	1997	Ranging	Success
MPL/DS2	1999	Profiling	Spacecraft lost
Icesat/GLAS	2003	Ranging / Profiling	
Calipso	2004	Profiling	
Messenger – Discovery Program Mercury mission	Future	Ranging	
DAWN – Ranging – Discovery Program asteroid mission	Future	Profiling	

The following guidance and navigation applications for LAMP are identified and discussed: 1) Capture of a Mars sample in Mars orbit. 2) Hazard avoidance sensor during smart landing on Mars. 3) Traverse planning for Mars rovers, 4) Rendezvous or docking with another spacecraft in earth orbit, 5) Small body landing/exploration/mapping.

1) Capture of Mars sample in Mars orbit: A future goal of the Mars program is to return a sample from Mars to Earth for detailed analysis. This is to be accomplished by sending

[1] 0-7803-7651-X/03/$17.00 © 2003 IEEE
[2] IEEEAC paper #1066, Updated December 11, 2002

a spacecraft to the Martian surface, which will collect a soil sample, package it into a grapefruit sized container covered with retroreflectors for ease of location and launch it into Mars orbit. Subsequently, a Mars orbiting spacecraft will use a LAMP system to locate and home in on the sample for capture and return to Earth. [3][4].

2) Hazard avoidance sensor during smart landing on Mars: Previous landings on Mars have utilized either radar-controlled retrorockets or airbags to land on comparatively flat terrains with minimal hazards. Future missions will require landings in more geologically interesting areas of Mars [5]. Therefore, a sensor that is able to guide the spacecraft away from large boulders and hazards on the martian surface in the final stage of descent is required. The LAMP sensor can make topographical maps of the surface with sufficient range and resolution to guide a lander to a safe landing spot.

3) Traverse planning for Mars rovers: The successful Mars Sojourner Rover and the twin Mars Exploration Rovers currently being built are using stereovision cameras to form 3 dimensional images of their proximity [6]. This approach only works in the daylight and has low accuracy at long distances. LAMP has neither of these limitations, enabling more capable path planning.

4) Rendezvous or docking with another spacecraft in Earth orbit: LAMP can be used as the terminal sensor for rendezvous with other spacecraft in Earth orbit. LAMP is planned to make a flight demonstration of this capability in the near term [2].

5) Small body landing/exploration: LAMP can be used as both a science instrument and a landing sensor on an asteroid or comet nucleus. LAMP can be used to generate a topographical map of the surface and determine the rotation of the body, and it can be used as a combined altimeter and hazard avoidance sensor during an actual landing [7].

A microwave radar system could also be used to support some of the same missions, but would require more resources (i.e. size, mass and power) and would provide poorer performance. The angular beam width of LAMP is designed to be only 0.02°, as compared to a typical 10° beamwidth of a microwave radar with a 10 cm aperture. In a rendezvous scenario, the larger beam width is not prohibitive, since it is possible to do loping to increase the angular resolution [8]. However, when generating a topographical map of a surface, the microwave-based radar has much lower resolution (or larger antennas).

2. LAMP SYSTEMS DESIGN

LAMP emits short, intense Q-switched pulses of infrared light, directed into the field by a lightweight rapidly steering 2-axis gimbaled optical mirror. When the light pulses encounter an object a portion of the pulses are scattered back, though the gimbaled reflector, into a 5 cm Cassegrain telescope. The range to the object is determined by measuring the elapsed time between the emission of the Q-switched pulse and its detection at the focal plane of the telescope.

A diagram of the LAMP system is shown in Figure 1. By sweeping the internal gimbaled mirror, it is possible to form a three dimensional image of objects in front of LAMP, similar to the operation of conventional pulsed radar [8].

The ranging laser on LAMP is a passively Q-switched Nd:YAG microchip laser. The pulse repetition frequency (PRF) is about 10 KHz and the pulse energy is about 10 μJ with a wavelength of 1064 nm. An external 2.5W pump diode laser at 808 nm is connected though an optical fiber to the microchip laser. The diode pump laser is housed in a separate thermally controlled package because its temperature must be maintained to within 0.3°C to efficiently pump the microchip laser. Temperature excursions exceeding this leads to poor absorption of the pump light and results in reduced microchip laser output. The laser beam emitted by the microchip is shaped by optics to have a 0.02° divergence.

When a laser pulse is emitted from the Nd:YAG microchip laser, some of the scattered light is detected by a fast Si-PIN detector, which starts a timer. A very fast Avalanche Photo Diode (APD) is mounted behind the classical Cassegrain telescope coupled to a series of high bandwidth amplifiers. When the light pulse returns, it generates a signal in the amplifiers that stops the timers when the signal crosses different thresholds. Since the dynamic range of the returned signal spans orders of magnitude a second Si-PIN detector is used to stop the timing chip when the APD approaches saturation. The timing chip has a clock frequency of 80 MHz, but is able to interpolate to a resolution of 390 ps, equivalent to ~2.5 GHz.

The 2-axis gimbal allows programmable, 2 axis motion of a 5 cm diameter beryllium mirror. It has an angular motion of 10° on both axes and a sweep rate of 10°/sec with the slow axis and up to 1000°/sec using the fast axis. Thus, it can scan a 10°x10° area in 1 second[3]. A Vertical Cavity Surface Emitting Laser (VCSEL) behind the scan mirror is continually reflected from the back of the mirror onto a position sensing detector (PSD). At the time that the laser pulse is emitted, the VCSEL spot on the detector unambiguously indicates the angular position of the scan mirror and consequently, the position in the field from which the pulse is returning.

[3] With the current beam divergence of 0.02 degrees, and a sampling rate of approximately 0.1 degrees spacing in both azimuth and elevation, a small grid of data points is generated which is representative of the surface topography, but could conceivable, miss small objects between the sample points. A simple solution to this is to expand the beam divergence, but at the expense of the maximum operating range.

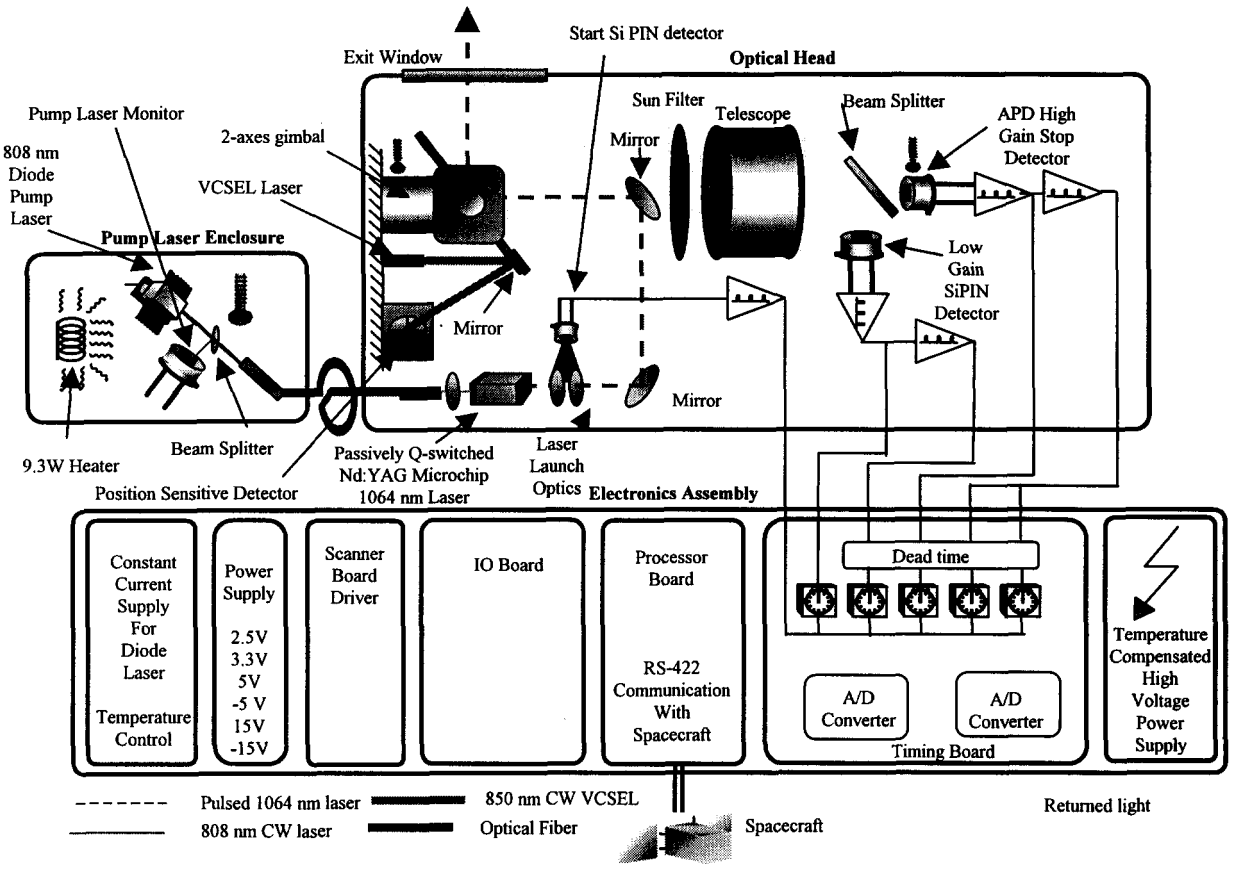

Figure 1 - LAMP block diagram

The LAMP processor is a 12.5 MHz, 32-bit MIPS R3000 Synova Processor with memory and RS422 interface. The processor controls the gimbal, monitors/controls temperature, reads the laser levels, reads the timing chip etc. The operating system is based on VxWorks. The processor/memory can accommodate various user applications. Table 2 summarizes key LAMP parameters and Figure 1 shows a block diagram of LAMP.

Table 2. Key LAMP parameters

Beam divergence	0.02°
Pulse repetition frequency	10 KHz
Mass	6.4 kg
Power consumption (without heaters)	33 Watts
Detection range (7 mm retro reflector)	>10 km
Detection range (lambertian surface)	2.5 km
Range accuracy	Offset: 10 cm +0.04% of range, random error 12 cm (3σ)
Sun exclusion angle	3°
Pointing accuracy	0.06° offset and 0.06° error (3σ)

3. LAMP PACKAGING

The LAMP Sensor consists of three separate units, the Optical Head Assembly (OHA), the Pump Diode Module (PDM) and the Electronics Assembly (EA). The function of the OHA is to transmit and receive a pulsed laser signal that scans over the field of view while the PDM houses a diode laser that provides continuous laser input to the microchip laser is located in the OHA. The PDM is isolated from the OHA because of a narrow-band temperature control requirement on the diode laser. Finally, the electronics assembly houses the driving electronics and the processor/communications.

The OHA consists of a chassis (optical bench), access covers and sub-assemblies responsible for performing the functions of the unit. The sub-assemblies include: laser launch optics, 2-axis gimbal, a telescope, detector assemblies, and passive optical elements. A rendering is shown in Figure 2 and a photograph is shown in Figure 3.

In addition to these major sub-assemblies, the OHA includes several minor components such as a solar filter, fold mirror, window, and scanner encoder. The solar filter is a piece of glass, with a diameter of 52 mm, located between the scanner and the telescope that only transmits laser light (and Sun light in a narrow band pass around the laser wavelength). The fold mirror, which is positioned along the telescope axis, directs the light at a 90° angle from the launch optics to the gimbal mirror. The window is a piece of sapphire glass that allows the laser beam to exit and enter the sensor. The window is tilted at an angle with respect to

the nominal optical axis to reduce the amount of back-scattered light into the telescope.

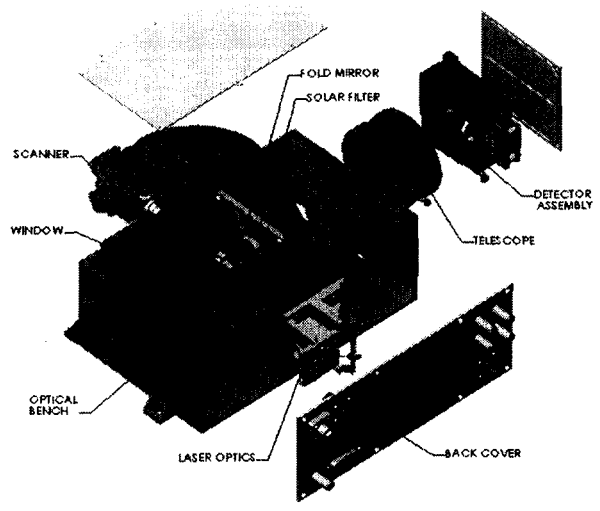

Figure 2 - Optical Head Assembly

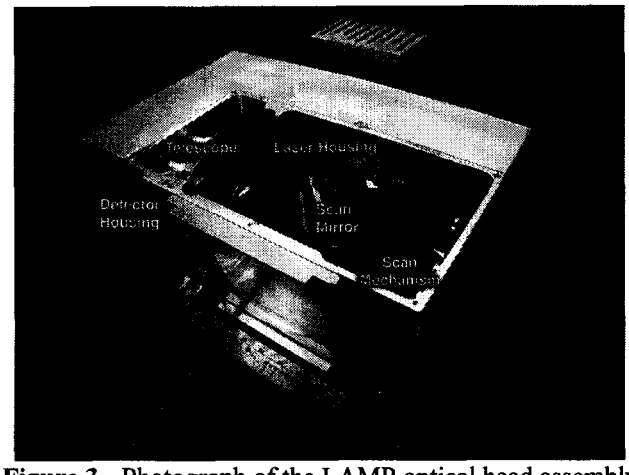

Figure 3 - Photograph of the LAMP optical head assembly without the top panel. The laser beam has been added for illustration.

The optical bench is the component to which all the parts and assemblies in the OHA mount. The optical bench also contains four mounting feet for mounting the OHA to the spacecraft. The optical bench is a single piece part machined out of a block of aluminum. The optical bench is designed to provide alignment stability for the optical elements when subjected to the thermal and structural environments of space missions. The back cover is the panel used to mount the electrical interfaces of the OHA. These electrical interfaces include connectors for the scanner, detector power and timing signals, and the fiber for the laser.

The second unit comprising the LAMP sensor is the Pump Diode Module (PDM). The PDM houses the laser diode that supplies the continuous laser input to the 1064 nm YAG crystal. The PDM is connected to the OHA via a fiber optic cable. The function of the PDM is to maintain the temperature of the laser diode within a narrow band about its nominal (20±0.3°C). The PDM consists of a housing, cover, laser diode, circuit card assembly, temperature sensor, heating element and connectors. The housing and cover are machined from aluminum and provide a thermally conductive path for dissipating the heat from the laser diode and heating element.

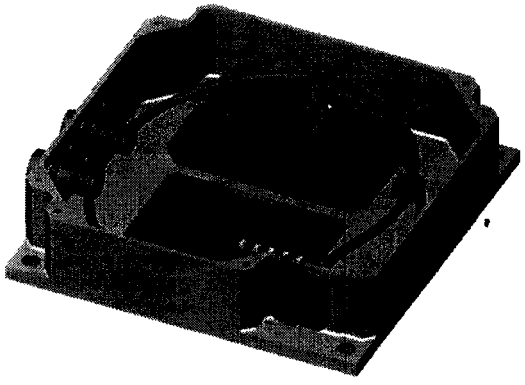

Figure 4 - Pump Diode Module

The Electronics Unit consists of seven electronic modules inside a machined aluminum housing. The modules are: processor board, I/O board, driver board for the scanner, timing board for measuring time of flight, power supply, current driver for the pump laser and high voltage supply for the APD detector. The backplane and module designs are based on the CompactPCI 3U Packaging Specification [9] and the I/O connectors are mounted on the front panels of the 3U modules. The unit is conduction cooled and the power dissipation of the unit is about 30 watts. Heat is transferred by conduction from the electronic modules to the unit housing via heat sink bars on the printed wiring boards. A rendering of the EA is shown in Figure 5.

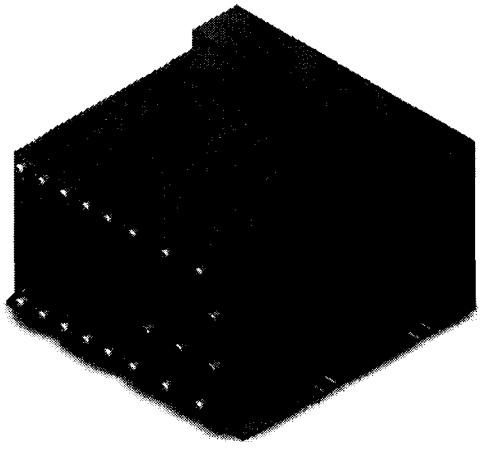

Figure 5 -Rendering of the electronics assembly

4. LASER TRANSMITTER

To meet the stringent power and thermal requirements of the system, the pump laser is thermally controlled with a large

radiator to space and a heating element. The temperature set point is 17°C-23°C with an accuracy of 0.3°C. A commercial fiber coupled pump laser with 2.5 W output from a 200-micron core fiber was chosen. The PDM maintains the temperature set point +/- 0.3°C to avoid changes in the wavelength. The pump laser is a standard 808 nm broad area laser diode that emits a multimode beam up to approximately 3 W continuous wave power. The device has an internal monitor photodiode for diagnostics as well as a thermistor temperature sensor for the closed loop temperature control.

The flight laser system will use an up-screened commercial part. The qualification and screening process has been tailored from Telcordia certification (GR 468-CORE) commonly used in power laser devices with some additional requirements due to the space environment. The main difference is the inclusion of radiation testing. Preliminary testing has shown that the overall laser system is not very susceptible to the radiation environment expected with any effects being annealed out at the higher optical powers. The fiber coupling to the laser head will also undergo pre-conditioning to ensure no degradation on orbit. A photo of the pump laser diode is shown in Figure 6.

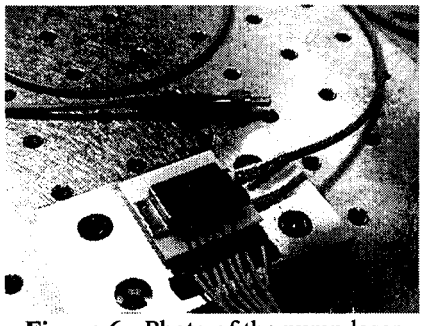

Figure 6 - Photo of the pump laser

LAMP requires a compact, lightweight pulsed laser transmitter with energy per pulse of 10 μJ at a PRF of ~10 KHz, a pulse-width rise time of less than 2 nsec, and no nulls in the far-field pattern of the beam. Stable average power, and low jitter and repeatable PRF are highly desirable. A passively Q-switched microchip Nd:YAG laser was selected as the laser transmitter. These lasers are simple, compact, and reliable sources with 1 to 100 kHz of PRF and nsec level pulses. The absence of control elements and continuous-wave laser pumping is a clear advantage of these lasers. The output wavelength depends on the host crystal used. Nd:YAG, Nd:YVO4 and Nd:LSB crystals were studied in detail along with a variety of passive Q-switched crystals including Cr:YAG. Based on the analysis, the requirements and on the commercial availability of the crystals with the required specifications, the Nd:YAG/Cr:YAG combination was selected. The pump diode is coupled to the crystal combination via a 0.29 pitch Graded Index (GRIN) lens. A sketch of the laser system is shown in Figure 7 and Figure 8 shows a photograph of the microchip laser.

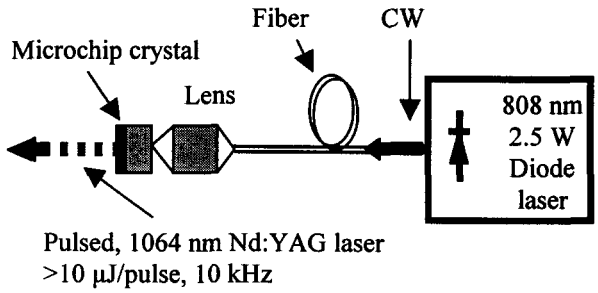

Figure 7 - Sketch of the laser transmitter

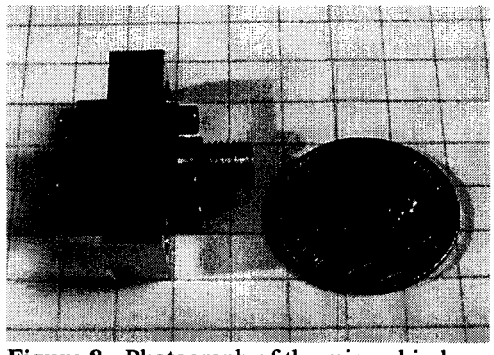

Figure 8 - Photograph of the microchip laser

A diagram of the LAMP optics is shown in Figure 9. The transmit optics consists of three elements that collect the output from the microchip laser and expand it up to provide a 0.35 mrad divergence output beam. This output beam is reflected off an adjustable turning mirror that is used for transmit/receive alignment. A second fixed turning mirror that is in the shadow of the secondary mirror reflects the beam onto an axis that is parallel to the receiver optical axis. The beam reflects off the scan mirror and is transmitted out to the target through a sapphire window.

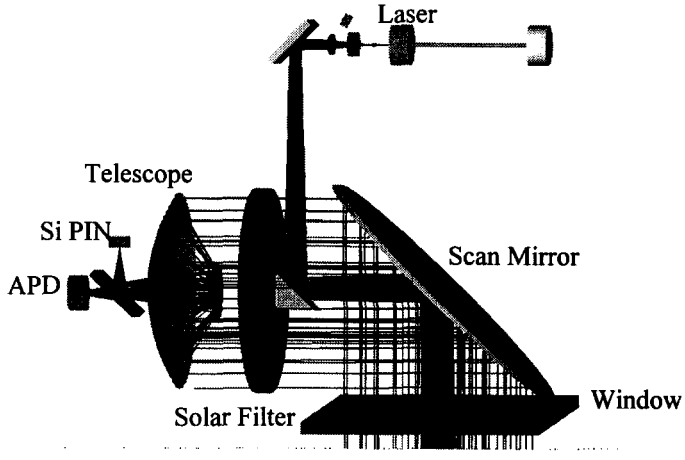

Figure 9 - Diagram of the LAMP transmit and receive optics

The laser launch optics is housed in a part referred to as the laser optics block. The laser optics block provides the mounting interface between the microchip laser, the optical bench and the laser launch optics. The axial position of the

convex lens (shown in Figure 10) is adjustable thus allowing one to optimize the laser beam. Lastly, the launch optics includes a tip-tilt adjustable mechanism to control the orientation of a 90° turning mirror. This adjustment is used to co-align the output beam from the sensor with the telescope axis. The alignment of the optics block is not sensitive to translation or to rotation about the axis of the output beam. However, the alignment is very sensitive to in-plane rotations of the optics block with respect to the output beam. The optics block mounts directly to the optical bench to provide a highly conductive thermal path for heat dissipated in the laser crystal. This mounting scheme provides adequate constraints on the two in-plane rotations. The last feature of the launch optics is the start-pulse detector located on a Circuit Card Assembly (CCA). This circuit will be described later in this paper. A rendering of the laser optics block is shown in Figure 10.

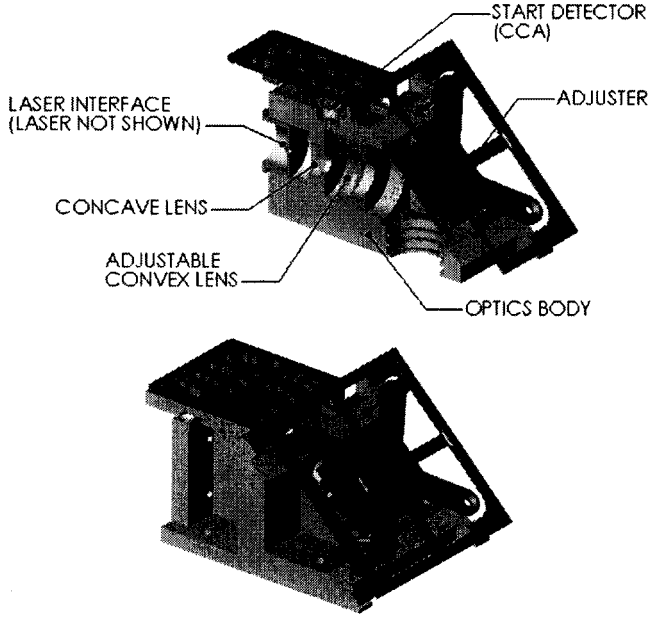

Figure 10 - Laser optics block

5. SCANNER

The purpose of the 2-axis gimbal (scanner) is to point the outgoing laser beam and collect the incoming reflected signal. The 2-axis gimbal consists of a mirror mounted to a yoke capable of rotating about two axes, azimuth and elevation. The mirror is nominally oriented at a 45° angle with respect to both the telescope axis and sensor output axis. The maximum angular range of the scan mirror about the azimuth axis, defined to be collinear with the telescope axis, is ±5°. The maximum rate of rotation about the azimuth axis is 1 Hz. The maximum angular range of the scan mirror about the elevation axis, which is normal to the plane defined by the azimuth axis and sensor output axis, is ±3° (since the laser beam is reflected off the mirror, this results in a range of ±6° for the beam). The maximum rate of rotation about the azimuth axis is 100 Hz. The angular motion of the mirror about both axes is controlled by a spring-actuator system. The springs are trefoil flexures integrated into the yoke that have a specified rotational stiffness (non-linear), while the actuators consist of coils and magnets. The electromotive force generated when current is applied through the coils creates a moment about the azimuth and/or elevation axis. The amount of current (proportional to the voltage across each coil) is proportional to the moment about each axis. The angular deflection about each axis is a function of the moment and the rotational stiffness. Therefore, the angular rotation about each axis is a function of the voltage across each set of coils. The 2-axis gimbal utilizes various materials to meet its functional requirements. The mirror is machined from beryllium to reduce mass and provide high stiffness. The magnets are neodymium-iron-born to produce a strong magnetic field for the coils. Finally, the yoke is made from titanium to optimize the stiffness, strength and fatigue properties of the trefoil flexures. A rendering of the scanner is shown in Figure 11.

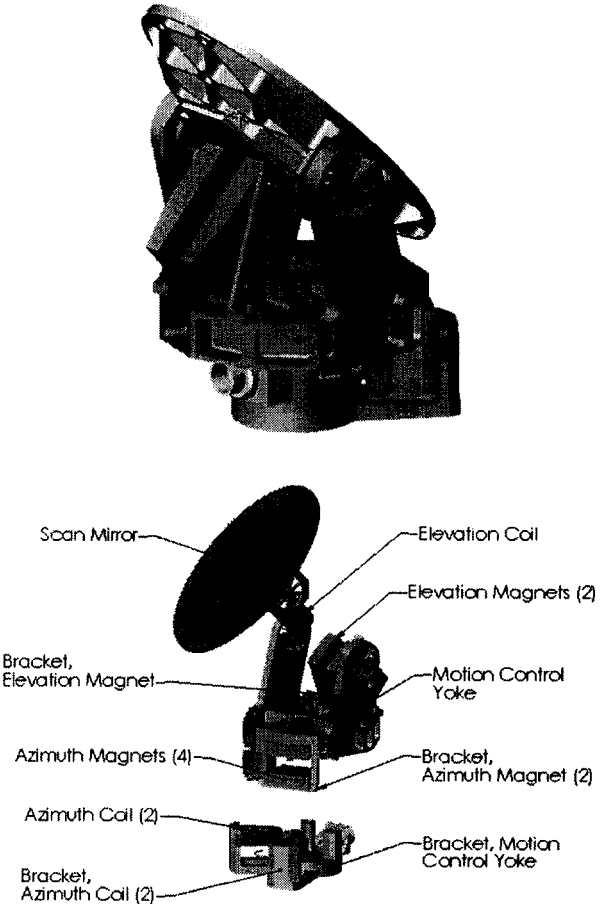

Figure 11 – Rendering of the 2 axis gimbal

The scanner board in the electronics assembly serves two functions. The first is to provide efficient drive for the slow and fast axes of the 2-axis gimbal assembly. The second is to monitor the position of the beam at all times since the 2-axis gimbal is operated in an open loop fashion.

The drive for the fast axis provides +/- 0.2A peak for the voice coil. This input in full scan mode is a triangular waveform that normally has a 20 ms period. A linear drive is utilized because of the relative low power level (as opposed to utilizing Pulse Width Modulation (PWM) based circuitry). The electronics protect the scanner from being driven against the mechanical stops. The slow drive signal is likewise triangular and has a period of 1 second in full FOV scans. A PWM drive signal for the slow axis is produced by the IO board. This simplifies the scanner board drive circuitry. The peak drive required by the slow scanner axis is +/- 0.7 A. A choice of two gain levels is provided to allow increased resolution at small angles.

The scanner encoder measures the angular orientation of the scan mirror by measuring the position of a laser beam reflected from a mirror mounted on the back of the scan mirror. A VCSEL is used to illuminate the scanning mirror. This was chosen because of the low optical power requirement, a reasonable beam quality and the fact that these types of lasers are very robust with extensive environmental testing being performed for the telecom market. The laser has a nominal output power of 1 mW at 850 nm and includes a monitor photodiode in a TO-46 can [10]. The light is reflected off of a small lightweight mirror mounted on the back of the gimbal mirror. The Position Sensing Detector (PSD) [11] is a 1 cm square, bi-lateral device. This detector senses the location of the focused VCSEL laser spot. The 4 outputs from the PSD are processed though 2 standard transimpedance amplifiers and 2 biased ones. The analog-processed data are sent to the I/O board and from there to the software that calculates the orientation of the outgoing beam.

6. LASER RECEIVER

The telescope assembly receives the incoming return beam from the scan mirror and focuses the beam onto the detector elements. The telescope assembly consists of five parts; barrel, primary mirror, secondary mirror support, secondary mirror and baffle. The challenge in designing this telescope was the requirement that the focal length be as short as possible to accommodate the tight packaging requirements of the sensor. The telescope receives a 50 mm diameter beam and focuses it on a spot approximately 15 mm behind the back surface of the telescope. The primary and secondary mirrors utilize bipod flexure mounting feet to create a statically determinant interface between the mirrors and the support structure. These features are necessary to relieve the mirror of any pre-loaded stresses during assembly that may deform the mirror surface. The telescope includes a means of adjusting the axial position of the secondary mirror with respect to the primary mirror. This adjustment, which consists of shims, barrel and secondary mirror support, is used to position the focal point of the telescope at the desired location. A rendering and a photograph of the telescope are shown in Figure 12.

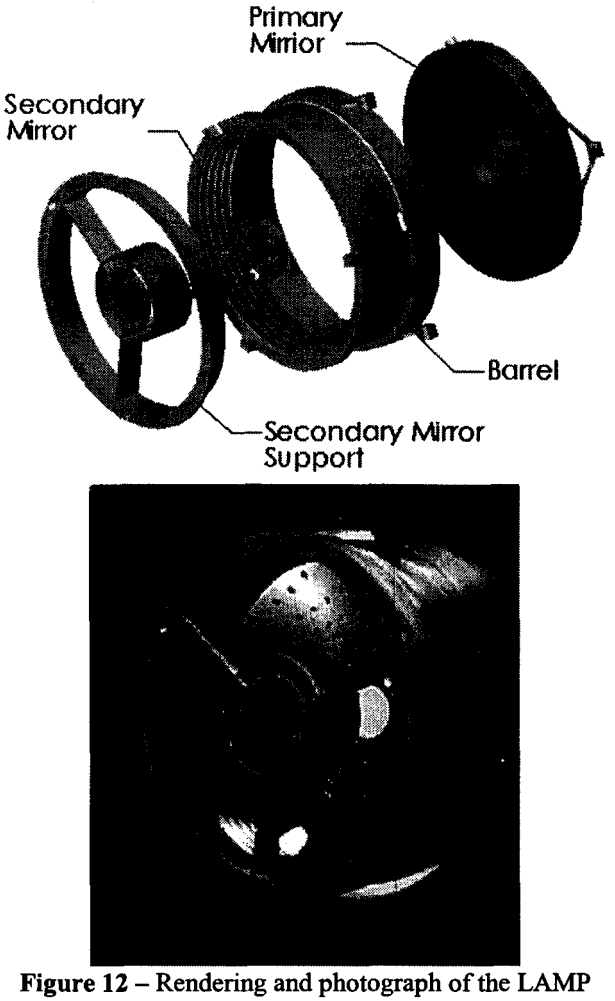

Figure 12 – Rendering and photograph of the LAMP telescope

As shown in Figure 9, the return signal passes back through the front window, off the scan mirror and through a 100 nm notch filter that minimizes the solar background. The signal then enters the 5 cm aperture F2.5 Casegrain telescope shown in Figure 12 that focuses the signal down onto the detectors. A beam splitter is used to split the stop pulse between two detectors.

The detector assembly consists of two CCAs, a beam splitter, and an adjuster mechanism. The detectors used to measure the incoming beam are located on each of the CCA's. The CCA's and beam splitter are mounted together such that the APD detector receives 99% of the light passing through the beam splitter, while the Si PIN detector receives the remaining 1% reflected light. Once assembled, the positions of the detectors and beam splitter are fixed with respect to each other. The detectors and beam splitter mount to an adjuster assembly that provides the interface to the optical bench. The adjuster provides translation of the detectors in all three axes, thus the detectors can be properly aligned with the focal point of the telescope. This is shown in Figure 13.

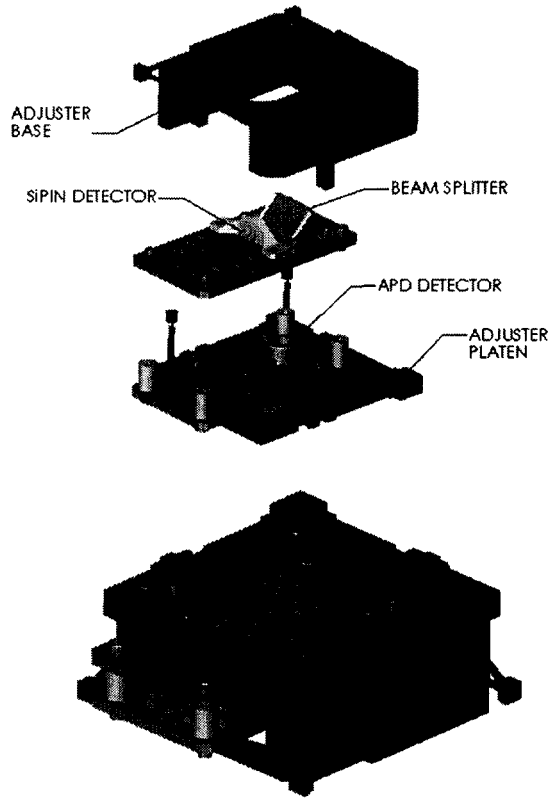

Figure 13 - Detector Assembly

The primary sensor is an Avalanche Photodiode (APD), which utilizes a strong electric field across the device to obtain an avalanche gain of approximately 200 to the return signal. This is necessary to amplify the return pulse sufficiently to meet the range requirements. The APD chosen for this application is the Perkin Elmer C30954E, chosen for its high quantum efficiency (~0.4) at 1064 nm, and its rapid response time of 2 nsec [12]. Both the gain and the breakdown voltage of this detector are strongly affected by temperature, requiring thermal monitoring of the APD and variable bias application to maintain a constant gain. The dark current at 20°C is 300 nA after receiving a total dose of 10 Krad(Si). The detectors were purchased in bulk, and tested and flight-qualified by JPL for optimal performance in the anticipated environment. At close range, the return pulse will saturate the APD. To meet the range resolution under these conditions, a silicon PIN detector with much lower quantum efficiency (0.05), but an equivalent 2 nsec rise time is used. The detector is model PSS 0.25-5 from Pacific Silicon Sensor. The same detector type is also used to sense the timing of the exiting laser pulse by observing the residual pulse light scattered by the optical surfaces of the transmitting optics in the laser optics block.

The APD receiver operates with approximately 300 volts reverse bias to provide the required amplification of ~200 for the electrons produced by the APD. Provisions are made so that it is possible to change the reverse bias to accommodate the temperature variations and to reduce the APD gain as the target gets closer to the instrument. The APD circuitry is shown in Figure 14.

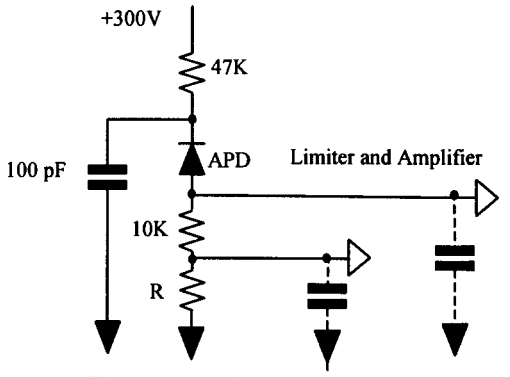

Figure 14 - The APD circuitry

The 47 KOhm resistor shown in Figure 14 is used to limit the APD current under condition of excessive amounts of light striking the APD. It also provides some protection to the APD if it inadvertently enters the Geiger mode. Also, it provides some filtering for the HV signal. The 100-pF capacitor serves to supply just enough energy to the APD to support "normal" level light pulses. The capacitance shunting the 10K resistor is due to the APD, the amplifier input, the Schottky diode limiter and to some parasitics. The total capacitance is estimated to be 4-5 pF resulting in a network bandwidth of 4 MHz (time constant ~40 ns). While the light pulse rise time is 2 ns, the narrow bandwidth of this network does not impact it, but it dramatically reduces the Johnson noise contribution of the 10K Ohm load resistor. The laser PRF is ~10KHz and is not impacted by the 40 ns time constant. The resistor R has a small value and is used to get a signal with lower amplitude. The output from the APD is fed to a 200 MHz low noise amplifier with a voltage gain of ~21. This is sketched in Figure 15.

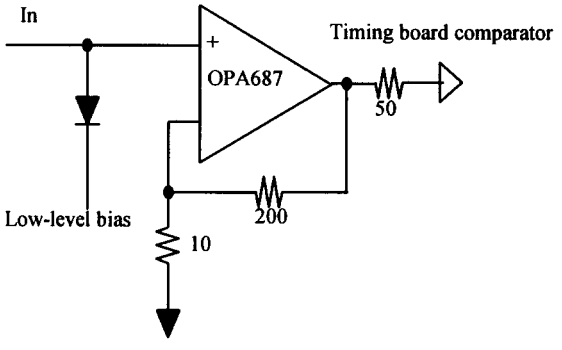

Figure 15 - The OPA687 amplifier circuitry

The OPA687 is configured as a voltage feedback amplifier with a gain bandwidth of 3.9 GHz, 0.9 nV/√Hz and 2.0 pA/√Hz noise. The thermal noise of the 10Kohm resistor is 26 μV_{RMS} [13]. The input referred noise of the amplifier is ~ 0.9nV/√Hz·√200MHz = 13 μV_{RMS}. The input referred current noise of the amplifiers is 2.5nA/√Hz·10KOhm·√4MHz = 50 μV_{RMS}. The S/N ratio will be discussed later in this paper. The output of the receiver is back terminated with 50 ohms and drives the

comparator/latch though a coaxial cable. In order to protect the receiver amplifier a Schottky diode is used across the input of the amplifier. Tests have shown that the diode is capable of protecting the amplifier chip.

When LAMP is ranging a bright close target, the APD will receive ~5 μJ pulses. This could potentially damage the APD and the receiver amplifier, but this is mitigated by reducing the high voltage reverse bias (under software control) to reduce the gain of the APD. This however, does not reduce the energy absorbed by the APD. Tests run of the APD with 10 μJ pulses has shown that the APD is immune to these short duration pulses and since the repetition rate is 10 kHz less than 100 mW is dissipated in the APD.

The Si PIN receiver and the start receiver are similar in design to the APD circuit. The demands on these circuits are much reduced and the detectors are operating at a few volts of reverse bias into a similar amplifier stage.

The timing board receives a "laser start" and five "laser stop" signals from the receivers in the optical head and produces 5 distances corresponding to the 5 "stops". The maximum distance measurement corresponds to ~470km. A block diagram of the timing board and the stop channels are shown in Figure 16.

The analog pulses coming from the optical head must be processed suitably before they can be used for the timing chip. The start pulse is level detected and is applied though a matched delay to the timing chip start input. The output of the start chip detector gates 4 of the 5 stop channels though AND gates. The delay can also be extended under the control of the IO board. The purpose of this delay circuitry is to prevent the output of the detectors from reaching the timing chip while the outgoing pulse is still being scattering in the optics. Efforts have been made to minimize the internal scattering in the optical head.

Stop channel #1 is treated differently than the other stops. Its output is not inhibited by the start detector output. Therefore the output of stop #1 is immediately available for the timing chip. This is used for short distance measurements. It gets around the internal scattering problem by having its threshold set higher than the largest scattering signal. The other four stop channels are used to measure ranges distant enough to allow the scattering to decay sufficiently as to not affect the system.

A scenario of a pulse coming from a great distance is shown in Figure 17. The Figure shows how the internal scattered light is gated out, and how the dim pulse returning is only bright enough to be detected by 2 of the 5 channels. Please note that due to the finite rise time of the laser, the stop pulse for stop #5 is generated a fraction of a ns before the stop of stop #4.

In Figure 17, it is observed that the timing of the stop pulses was not simultaneous, but was different at the ns level. This information can be used to infer the brightness of the pulse and thereby improve the range estimate. The two highest gain signals are integrated and processed by 2 A/Ds to provide intensity information about the targets. Emphasis was placed on delay tracing within the timing board and a temperature sensor, which allows for calibration of the channels output vs. temperature.

The functionality of the timing chip resembles 5 stopwatches. The timing chip could in principle be implemented using a 2.5 GHz accurate and highly stable oscillator and a binary counter for each channel. However, such a design is difficult and would have a very high power consumption of several watts. Also, Meta stable errors would be quite numerous at such a high frequency. (Meta stable errors stem from the asynchronous relationship between the local clock and the arrival of the laser pulses.)

The timing chip was custom made at the Technical University of Oulu [14]. The chip is free of Meta stable errors and has an LSB resolution of 390 ps at a power consumption of 100 mW. The chip is designed by creating a 32-bit stage phase locked loop, which is synchronized with the 80 MHz[4].

The timing chip is used to estimate the fraction of a clock cycle not captured by counting the elapsed time between outgoing and return pulses using an 80MHz clock. When the timing chip estimates the elapsed time between start and stop, it counts the time using the 80MHz clock. However, when it encounters the start pulse, it also reads the start interpolation register that contains information on the position of the traveling wave. The same thing happens when the stop signal is encountered. This whole process is illustrated in Figure 18.

7. DIGITAL ELECTRONICS

The Lamp Processor is a radiation hardened R3000 microprocessor that has 4 Mbytes of EEPROM memory and 64 Mbytes of SDRAM memory. At its maximum processor speed of 12.5 MHz it has a throughput of 10 MIPS. The software programmable clock rate feature allows for the system clock to be divided down to as low as ~100KHz which enables approximately a factor of 100 in power savings. Along with the processor and memory the board has an 8 channel DMA FPGA that is utilized to communicate with the I/O board. The serial interface FPGA can be programmed for synchronous or asynchronous protocols up to 4 Mbits/second. Software reset capability and a watchdog timer are implemented. The processor board is a 3U card

[4] In other words to put 32 digital buffers in series and have a clock signal propagate though the buffers as a "wave"

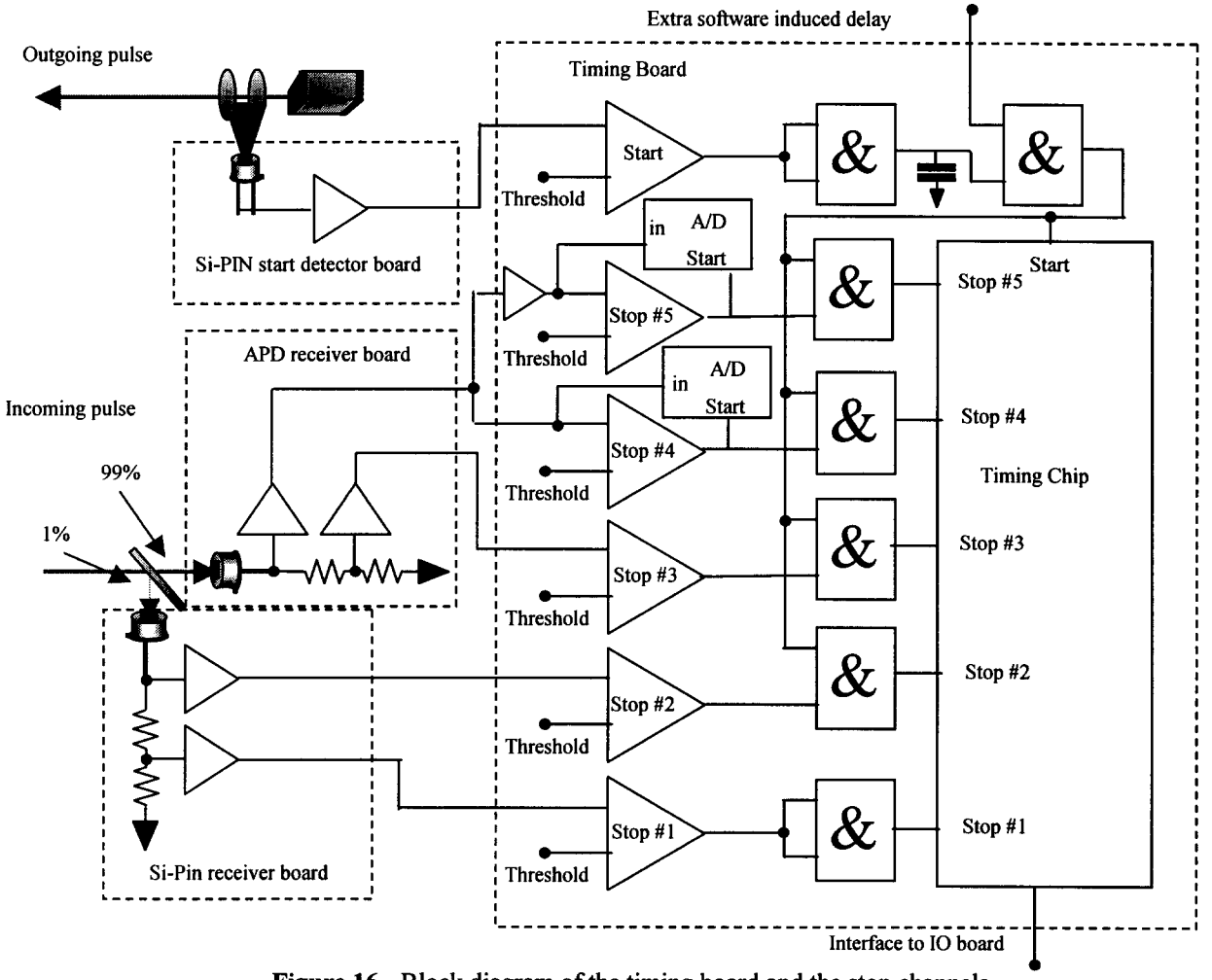

Figure 16 - Block diagram of the timing board and the stop channels

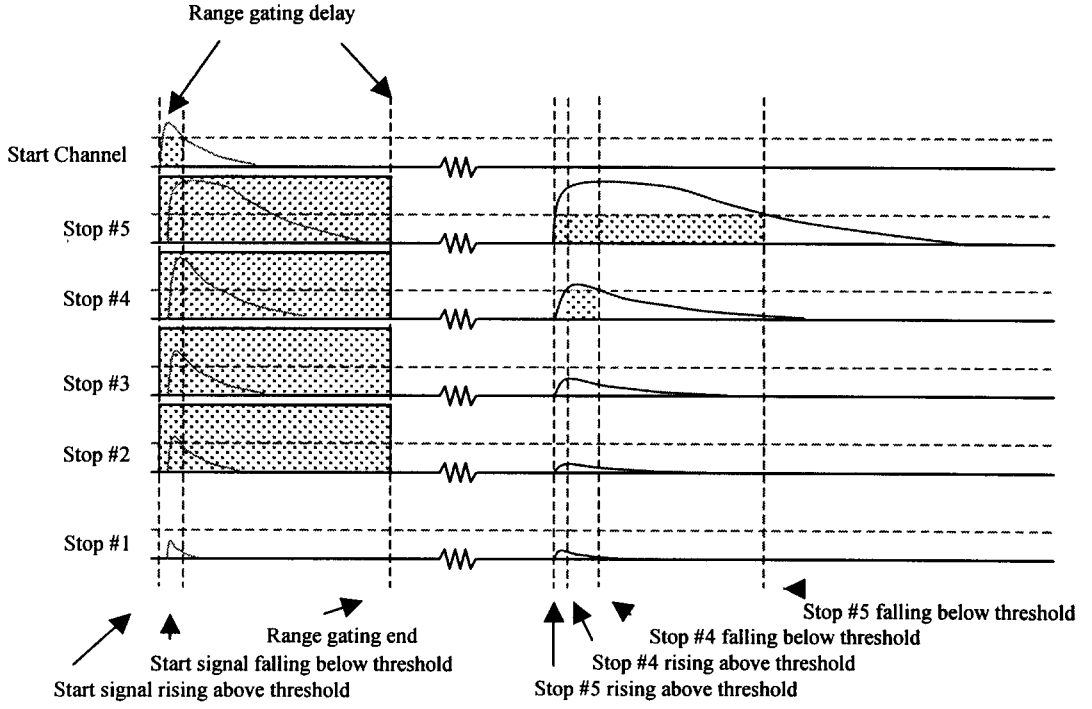

Figure 17 - Signals and timing diagram when receiving a dim pulse

format and has a nominal power draw of 2.9 watts at the maximum system clock and the serial and backplane DMA features running. A block diagram of the processor is shown in Figure 19. Board capability is summarized in Table 3.

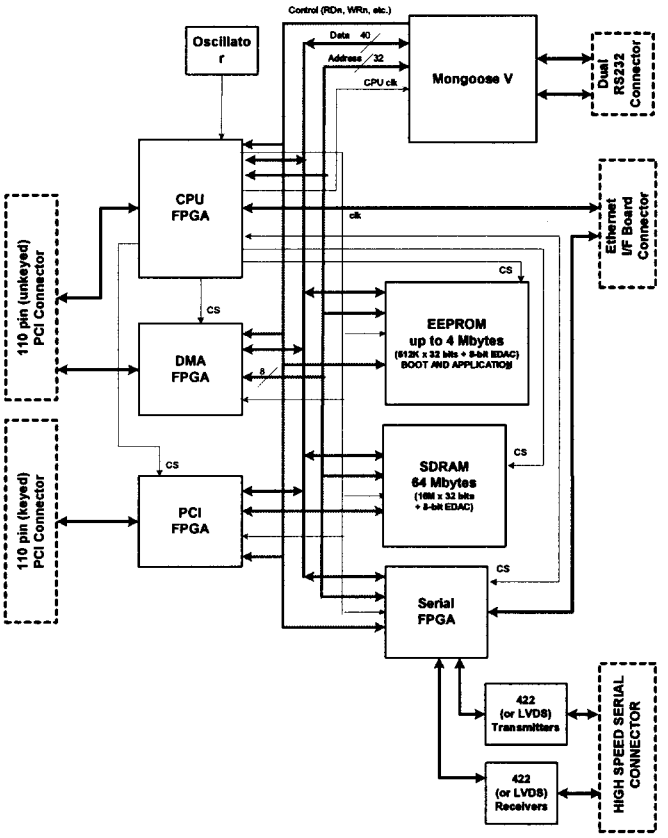

Figure 19 - LAMP Processor Board Block Diagram

The I/O board provides all interface connections from the processor to the rest of the system. The only communications to the processor is through direct memory access port with 4 I/O request/grant channels. All instructions come through this port. The I/O board provides the horizontal and vertical scanning capability, which is driven through DMA instructions. The horizontal axis output is through a 12-bit D/A with a +/- 5V drive. The vertical axis is through a PWM output. All other output is through the digital control output word. Onboard input and output FIFO's help reduce the amount of DMA activity.

Inputs are read from the timing board and assembled into the round trip time information of the laser pulse. Two A/D converters are used to read the gimbal mirror angles along with other voltage and temperature data. This data is read when the laser fires and sent back though the DMA port to the processor along with a time tag. A block diagram of the I/O board is shown in Figure 20.

The LAMP processing architecture is designed to support the different applications described in the beginning of this paper. The processor has sufficient computational power to process 10,000 3D points per second. This data can be used to determine relative motion between the spacecraft and a body (Mars landing, small body rendezvous), hazard evaluation (landing), surface mapping, or to support rendezvous operations (acquiring and tracking of a spacecraft/object). LAMP is also capable of transferring all collected data (via a serial port) to the spacecraft for further analysis or download.

8. SOFTWARE SUBSYSTEM

The software is functionally divided into two parts. An application specific process(es) that directs the data collection effort (when and how to scan), processes the data to retrieve relative motion information or hazard locations, and sends the information/data to the spacecraft via the serial port. The application software sits on top of a set of generic software routines called LAMPOS. LAMPOS provides the device drivers and auxiliary routines needed for communication and to control the LAMP hardware (power control, scanner control, IO operations, data formatting and movement). In addition, LAMPOS has routines that allows for sharing resources and providing process controls (starting and ending process, intra-process communication, clean-up, etc.).

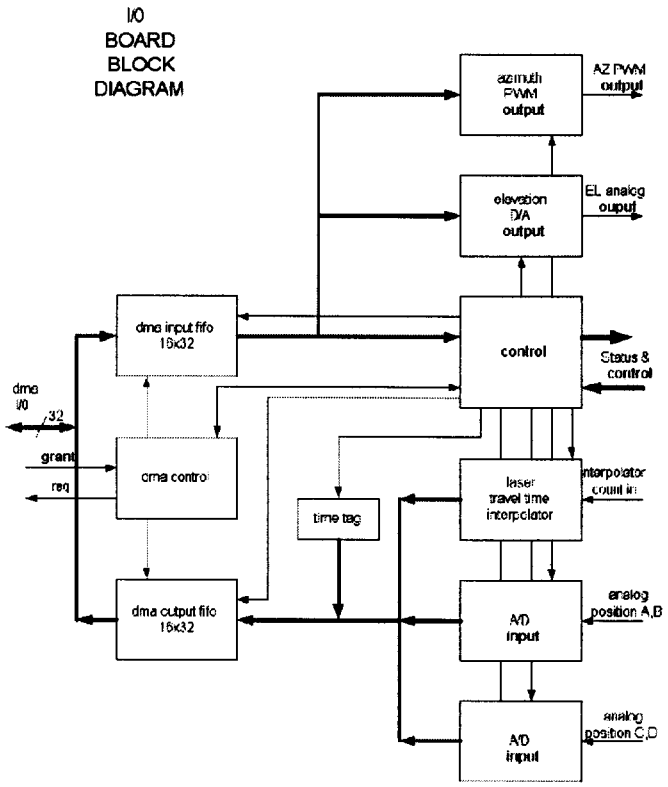

Figure 20 - Block diagram of the I/O board

9. POWER SUBSYSTEM

The power subsystem consists of three main components: The digital and analog power converter, the current source power supply and the high voltage power supply. The digital and analog power converter consists of 5V, 3.3V and 2.5V,

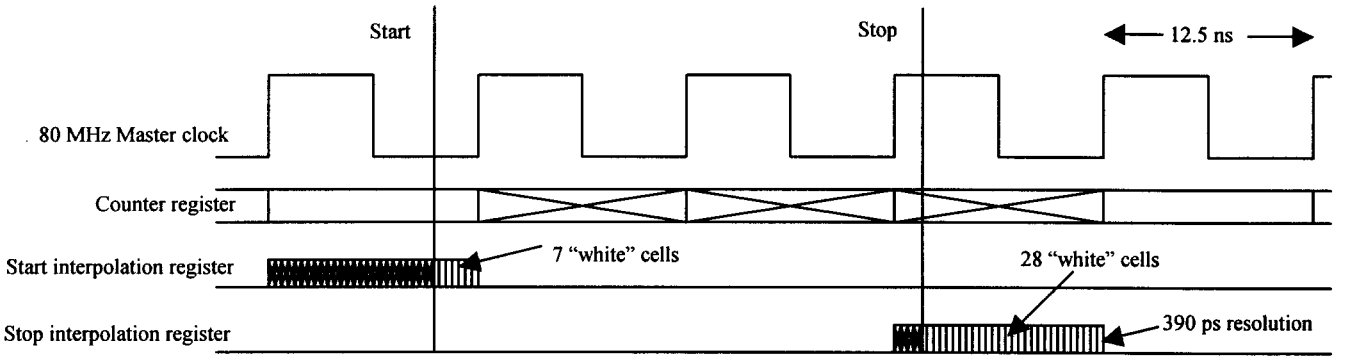

Figure 18. Timing estimation, Elapsed time: 3 * 12.5 ns + 7 * 390 ps - 28 * 390 ps = 29.31 ns

Table 3 LAMP Processor Board Capabilities Summary

Processor	12.5MHz	10MIPs	Rad Hard
SDRAM	64Mbytes	EDACed	20Krad
EEPROM	4Mbytes	EDACed	40Krad
RS-232 UARTS	2 Channels	38Kbits/sec	Rad Hard
RS-422 Sync	1 Channel downlink	1.5Mbits/sec	100Krad
RS-422 Async	1 Channel Uplink	480Kbits/sec	100Krad
DMA	8 Channel	12Mbytes/sec	Rad Hard
Watch Dog Timer, Software programmable system clock and Reset			

which provide power to the digital circuits, and low noise ±5V and ±15V provide power to the analog circuits. It receives its input from the spacecraft 28V bus. In addition to DC/DC power converters, it also provides control circuitry for synchronization, ON/OFF command for the analog converters, temperature sensing, under voltage detection and slow start circuit to reduce input surge current. The current source power supply provides constant current for the pump laser. The control circuitry includes 5 digital bits to adjust output current, ON/OFF command and temperature sensing. The high voltage power supply is an adjustable voltage supply, which provides voltage to the APD. It can supply voltages up to 500V and 1 mA of current. The control circuitry consists of 2 digital bits to adjust the output voltage and temperature control to compensate the output voltage.

10. ESTIMATED S/N RATIO

This section will show a calculation of the expected signal to noise ratio in LAMP. A scenario, when ranging a single 7-mm retroreflector at a distance of 5 km was chosen. The scenario is relevant for Mars applications when trying to detect an orbiting sample canister as discussed in the introduction of this paper. In Table 4 is shown a "photon budget" and different signal levels in Volts.

Table 4. Signal to noise ratio terms for ranging a retroreflector

	Signal	Value	Unit
1	No. photons in pulse emitted from LAMP	2.41E+13	Photons
2	No. photons intercepted by 7mm retroreflector	3.85E+08	photons
3	Backscattered photons on intercepted by detector	1.01E+05	photons
4	Photoelectrons generated by laser pulse	1.42E+06	Photo electrons
5	Voltage generated by laser pulse	5.04E-02	Volt
	Noise		
6	Photon noise	5.99E-04	Volt
7	APD gain noise	3.56E-03	Volt
8	Dark current	1.96E-05	Volt
9	APD noise	7.00E-04	Volt
10	Johnson Noise	2.60E-05	Volt
11	Input referred amplifier noise	1.27E-05	Volt
12	Input referred current noise	5.00E-05	Volt
13	Sun induced background signal	1.95E-05	Volt
14	RSS of noise voltages	3.68E-03	Volt
15	S/N	13.7	

The following explanation is given for the numbers in Table 4:

1) The laser pulses are 10 μJ at 1064 nm. It is assumed that 50% of the photons are lost in the launch optics and 90% are transmitted though the exit window.
2) The outgoing beam divergence is 0.35mrads. This result in a beam area of 2.4 m^2 at 5 km. Therefore, only $1.6 \cdot 10^{-5}$ of the photons will intercept a 7mm diameter retro reflector.

3) The photons intercepted by the retroreflector have a very small beam divergence, but due to diffraction the 7mm retroreflector results in a 0.39 mrad returning beam divergence. Also, it is assumed that only 80% of the photons are transmitted in the retroreflector. The returning beam has an area of 3.1 m^2 at LAMP. The telescope has an aperture of $1.8 \cdot 10^{-3}$ m^2. Also, it is assumed that 10% of the photons are lost in the front window, 69% is transmitted in the telescope and 90% is transmitted though the solar filter.

4) The shape of the laser pulse is that it rises sharply and has a much slower decay. In order to achieve accurate timing of the pulse, it is desirable to detect the pulse at the sharply rising part of the pulse. Therefore, it is required to detect the first 20% of the pulse. Also, only (conservative) 35% of the photons are converted into photoelectrons in the APD detector. The detected photoelectrons are on average multiplied with 200 in the APD diode.

5) The pulse coming from the APD is stored in a 4.5 pF capacitor (as shown in Figure 14).

6) The photoelectron noise is the square root of the detected photoelectrons multiplied by 200 (gain in the APD) and converted to a voltage over the 4.5 pF capacitance.

7) As a first order approximation it is assumed that the gain noise of the APD is square root of 200 = 14 photoelectrons. This noise is generated for every single photoelectron and converted into a voltage.

8) The dark current of the APD at 40°C and after having received total radiation dose is less than 3 μA. The bandwidth is 4MHz. Therefore the dark current noise is $\mathrm{sqrt}(2 \cdot e \cdot I_{DC} \cdot B) = 2\text{nA}$ or 19.6 mV [15].

9) The APS noise is less than 35 pA/sqrt (Hz). The input bandwidth of the APD amplifier (shown in Figure 15) is 4 MHz.

10) Johnson noise over a 10 KOhms resistor with 4 MHz bandwidth [13].

11) Described under APD previous

12) Described under APD previous.

13) In this number it was assumed that the sun is shining on the front glass (but outside the 3°-exclusion angle from the sun). 10% of the sun is absorbed in the front glass and re-emitted homogeneously in all directions. Some of this light reaches the detector. The DC value is converted into a voltage.

14) The noise sources are RSSed together.

15) The signal to noise is 13.7, which is sufficient to detect a signal. It is observed that the dominant noise source is the APD gain, which is proportional to the signal. This means that LAMP has much longer detection range. Redoing the entire calculation shows that the S/N at 10 km is still >4.

11. SUMMARY

This paper has described a laser radar that is being developed at JPL. The laser radar is designed as guidance and navigation sensor for rendezvous, landing and traverse planning applications. It will form a 3 dimensional image of its field of view. A block diagram of the sensor is shown and the overall system design is discussed. LAMP consists of 3 individual boxes: 1) an optical head with gimbal, lasers, optics and detectors. 2) Electronics Assembly consisting of the processor, I/O boards, power supplies, drivers and timing board. 3) A small module containing the pump laser that has its temperature controlled very accurately. The laser transmitter consists of an 808 nm diode pump laser that pumps a passively Q-switched Nd-YAG laser. When the laser pulses leave the sensor, they bounce off a beryllium mirror that determines the orientation of the beam. The outgoing laser pulses will hit a target and a small fraction of the pulse will be scattered back to the sensor, where it is collected by a telescope and detected by an APD detector. The time of flight is proportional to the distance to the target and registered for all points. The signal to noise ratio achieved in LAMP is also discussed.

REFERENCES

[1] D.Tratt, R. Menzies, R.Bartman, H. Hemmati: Scanning Laser Radar Development for Solar System Exploration Applications, 20th International Laser Radar Conference, Vichy, France, July 10-14, 2000.

[2] R.P.Kornfeld et al: New Millennium ST6 Autonomous Rendezvous Experiment (ARX), Paper accepted at the 2003 IEEE Aerospace Conference, Montana March 2003.

[3] Christian Cazaux et al: The NASA/CNES Mars sample return - A status report, Source IAF, International Astronautical Congress, 52nd, Toulouse, France, Oct. 1-5, 2001,

[4] D. Clouse et al: Covering a sphere with retroreflectors, 2001 IEEE Aerospace Conference, Big Sky, MT, Mar. 10-17, 2001, Piscataway, US, IEEE, 2001, p. 1495-1506.

[5] Mars Technology Program, Proceedings of i-SAIRAS 2001, URL: http://www.space.gc.ca/csa_sectors/generic_space_tech/spa_craft_eng/rob_aut/isairas/default.asp, cited 11/18/02.

[6] A.Eisenman et al: Mars exploration rover engineering cameras, Fifth Conference on Sensors, Systems, and Next-Generation Satellites, Toulouse, France, Sept. 17-21, 2001, Bellingham, WA, Society of Photo-Optical Instrumentation Engineers, 2001, p. 288-297.

[7] T.D.Cole: NEAR Laser Rangefinder: A tool for the Mapping and Topologic Study of Asteroid 433 Eros, URL: http://pdssbn.astro.umd.edu/NEARdb/documents/nlr/nlr.pdf, cited 11/18/2002.

[8] G.W.Stimson: Introduction to Airborne Radar, SciTech Publishing Inc., ISBN: 0-7803-3491-4.

[9] PICMG 2.0 Revision 3.0 dated October 1, 1999. PCI Industrial Computer Manufacturers Group (PICMG) PICMG, 401 Edgewater Place, Suite 500, Wakefield, MA 01880 USA, URL: http://www.picmg.org

[10] URL: http://content.honeywell.com/vcsel/products/datacom.stm, http://www.emcore.com/PDF/TO-46.PDF, cited 11/18/01

[11] Sitek, Sweden: URL: http://www.sitek.se/pdf/psd/2l10sp.pdf, cited 11/18/02

[12] Perkin Elmer: URL: http://opto.perkinelmer.com/producttemplates/SubCat2.asp?levelId=14494&s=2&ss=1, cited 11/18/02
[13] E.A Bahaa et al: Fundamentals of Photonics, Wiley-Interscience; ISBN: 0471839655;
[14] University of Oulu, Finland: URL: http://www.infotech.oulu.fi/Annual/1999/HSELE.html, cited 10/2/02
[15] P.Horowitz and Winfield Hill: The art of electronics, Cambridge University Press, 1989, ISBN:0-521-37095-7.

ACKNOWLEDGEMENT

The authors of this paper would like to thanks the Mars Technology Program at the Jet Propulsion Laboratory, California Institute of Technology for providing the funding for this work.

The research described in this paper was carried out at the Jet Propulsion Laboratory, California Institute of Technology and was sponsored by the National Aeronautics and Space Administration. References herein to any specific commercial product, process or service by trademark, manufacturer, or otherwise, does not constitute or imply its endorsement by the United States Government or the Jet Propulsion Laboratory, California Institute of Technology.

BIOGRAPHIES

Dr. Carl Christian Liebe received the M.S.E.E. degree in 1991 and the Ph.D. degree in 1994 from the Department of Electro physics, Technical University of Denmark. Since 1997, he has been an employee at the Jet Propulsion Laboratory, California Institute of Technology. Currently, he is a senior member of the technical staff in the Precision Motion Control Systems and Celestial Sensors Group. His research interests are new technologies and applications for avionics sensors. He is the systems engineer for LAMP. He has authored/co-authored more than 40 papers.

Dr. Alex Abramovici received a Ph.D. in physics from the Weizmann Institute of Science, Israel in 1985. Has joined JPL in 1996. He has worked on ground-based interferometric gravitational wave detectors, and on airborne and space based laser metrology and interferometry measurements. Alex is responsible for the LAMP signal electronics.

Randy K. Bartman received a B.S. degree in physics from California Institute of Technology in 1977. At which point he became an employee of the Jet Propulsion Laboratory. Randy Bartman is the deputy section manager for the Interferometry Systems and Technology Multidivisional Section. His research interests include lasers, and interferometry. Randy is the chief engineer for LAMP.

Robert L. Bunker is a graduate of the California Institute of Technology, and has spent the last 33 years at JPL designing and managing spacecraft avionics systems, including more than 10 years in line management of flight avionics systems. His experience includes spacecraft computer systems, advanced VLSI and system design for radiation and Single Event Effects environments, and celestial sensors used for spacecraft attitude control. He has worked on Mariner, Viking, Voyager, Galileo, Cassini, Mars Global Surveyor and Mars Odyssey spacecraft, as well as providing guidance and leadership for JPL institutional programs in flight VLSI design and model based spacecraft system/subsystem design methodologies. Mr. Bunker is a Principal Engineer and has received recognition for his innovative contributions to the interplanetary program and has authored several papers on advanced electro-optical sensors and computers for use on planetary spacecraft. Currently, Mr. Bunker is the Project Manager for the Autonomous Rendezvous Experiment (ARX) and the Laser Mapper (LAMP) development, which is the flight sensor used by ARX.

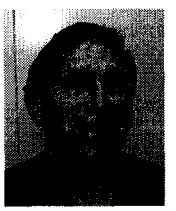

Jacob Chapsky is a senior electronics design engineer with 46 years of experience in designing military, space and industrial subsystems. He has an M.S.E.E. degree from USC. He was a chief scientist at Hughes Aircraft where he was responsible for many space-deployed subsystems. As a principal engineer at California Institute of Technology he played a critical part with his designs in achieving the $2 \cdot 10^{-9}$ m/$\sqrt{\text{Hz}}$ noise floor for the Gravitational Wave detector. He was also a program engineer for 2 Apollo instruments deployed on the Moon in 1969. Jake is working on the LAMP signal electronics.

Dr. Cheng-Chih Chu is the Group Supervisor of Simulation and Verification Group at JPL, responsible for the development and implementation of simulation tools and verification process for the avionic subsystem in support of various JPL missions. Dr. Chu received his M.S. degree in Electrical Engineering and Ph.D. degree in Control Science from University of Minnesota in 1985. He has 18 years of extensive experience in program and technical management, GNC system design and analysis and has authored over 40 publications. As the assistant program manager for NASA's Mars Technology Program at JPL he initiated the LAMP project

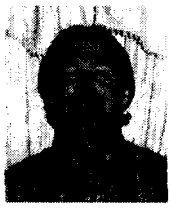

Dr. Daniel Clouse received the B.A. degree in Computer Science from the University of California, Berkeley in 1982, the M.S. degree in Computer Science from the University of California, San Diego (UCSD) in 1992, and the Ph.D. degree in Cognitive Science and Computer Science from UCSD in 1998. He is a Member of the Technical Staff at the Jet Propulsion Laboratory, California Institute of Technology in the Machine Vision group of the Mobility Section. His interests include vision processing, neural networks, language translation, and word sense disambiguation. Dan is responsible for the LAMP software.

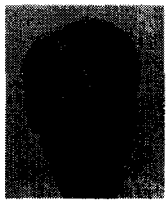

James W. Dillon, Received his BSEE in 1967 from Indiana Institute of Technology. He came to JPL in 1974 and worked many projects including VLBI (very long baseline interferometry), The Human Genome Project, Hypercube, Cassini, and Pathfinder. He is a Senior Engineer in the Electronics Design group and is currently doing the Processor I/O board design for LAMP.

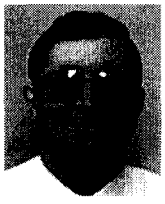

Bob Hausmann has over 40 years experience in the mechanical design and electronic packaging of defense and aerospace electronic systems. He has directed packaging engineering activities on shipboard, aircraft, land based vehicles, and space electronic systems. He is currently a senior engineer in the Electronics Packaging and Manufacturing Section at the Jet Propulsion Laboratory and has led electronic packaging teams on the Cassini, Cloudsat, and LAMP Programs. Bob has a BSME degree from California State University – Los Angeles and an MBA degree from California State University – Fullerton. He is an active member of the IMAPS and SMTA engineering technical societies and a senior member of the IEEE.

Dr. Hamid Hemmati, Ph.D. Physics 1981, joined JPL in 1986 and is now supervisor of the Optical Communications Group. His research field includes: free-space laser-communications, solid-state lasers and electro-optical instrumentation. He has been involved in several space laser experiments, including the GOPEX project, the Japanese laser communications experiment, and LAMP/ST6 project. Hamid is responsible for the microchip laser.

Dr. Richard P. Kornfeld received a Diploma (M.Sc.) in Electrical Engineering from the Swiss Federal Institute of Technology (ETH) in Zurich, in 1994 and a Ph.D. degree in Aeronautics and Astronautics from MIT in 1999. In 1994-1995 he was with McDonnell Douglas Aerospace (now Boeing) in St. Louis, Missouri. Since 1999 he has been at the NASA/Caltech Jet Propulsion Laboratory where he is a Senior Engineer in the Advanced Concepts and Architecture Group in the Avionic Systems Engineering Section. He currently serves as the ARX/LAMP Project Engineer and ARX Lead Systems Engineer.

Clint Kwa received his B.Sc. and M.Sc. degrees from University of Southern California in 1975 and 1976 respectively. He has held various engineering positions in commercial industries. He joined JPL in 1990; his involvement includes Drop Physic Module, Cassini and TES programs. In 1999, he joined the Power and Sensor Electronics Section at JPL as a Senior Engineer. Clint is responsible for the LAMP power supplies.

Dr. Sohrab Mobasser received his Ph.D. from Stevens Institute of Technology at New Jersey in experimental solid-state physics in 1982. He is a Senior Member of the Engineering Staff at the Jet Propulsion Laboratory, California Institute of Technology. Sohrab has more than 18 years of aerospace industry experience, most of it in spacecraft attitude determination. His work can be found on many planetary missions, from the Galileo mission to Jupiter to the successful Pathfinder mission to Mars and the Cassini mission to Saturn. His current interests are new technology and applications for autonomous attitude determination. Sohrab is responsible for LAMP I&T.

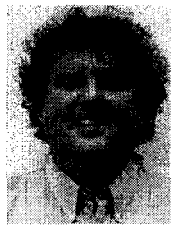

Michael Newell has seventeen years of experience designing and analyzing digital and analog systems for space flight. His flight work includes design of integrated circuits design for the Cassini Spacecraft, lead designer of the APEX flight experiment, avionics lead of the Deep Impact project along with design analysis on the Sojourner Rover. In addition to his work in Flight Avionics, he has been investigating operation of CMOS devices at cryogenic temperatures for use in space for the past seven year. He is the task manager of extreme temperature electronics in the NASA Electronics Parts Program. He has a patent and a NASA Space Act Award for his work on a space 32-bit risk processor MCM with reconfigurable hardware. He has a BSEE from the California State Polytechnic University, Pomona. Mike is the hardware lead engineer on LAMP.

Dr. Curtis Padgett received his Ph.D. from the Computer Science and Engineering Department at the University of California at San Diego (UCSD) in 1998. He received his M.S. degree from the same department in 1992. He has been employed at the Jet Propulsion Laboratory, California Institute of Technology, Pasadena since 1993. He is a Senior Member of the Technical Staff in the Machine Vision group of the Mobility Section where he works on remote sensing applications for space systems. His research interests include algorithm optimization, machine vision, and artificial intelligence applied in classification and pattern recognition tasks. Curtis is the software lead engineer on LAMP.

Dr. W. Thomas Roberts received a B.Sc. (1981) and a M.Sc. (1985) from The University of Alabama and then worked at the Nichols Research Corporation. He moved to the Optical Sciences Center, University of Arizona in 1994 where he got the M.Sc. in 1996 and the Ph.D. in 2001. Tom has been employed at the Jet Propulsion Laboratory, California Institute of Technology, Pasadena since 2001. He is currently a Senior Member of the Technical Staff in the Optical Communications Group where he works on developing high-efficiency Q-switched Nd:YVO4 lasers for deep-space optical communication and is the cognizant engineer for the LAMP detectors. Tom is the author of papers in magnetospheric physics, Radiometric Analysis, Satellite Sensor Characteristics, Infrared Detector Development, and Guide Star Laser Development.

Gary Spiers is the Acting Supervisor for the Laser Remote Sensing Group at JPL. He currently holds a Lidar related visiting scientist position with UCAR and is a member of a number of Lidar working groups and committees. Prior to joining JPL he was the Coherent Lidar Systems Engineer for the EO-2 Space Readiness Coherent Lidar Experiment (SPARCLE) and participated in other earlier Doppler wind Lidar efforts at NASA MSFC. He received his BSc degree in physics and his MSc in Lasers and their applications in 1984 and 1985 respectively from Essex University, England. Between 1985 and 1990 he carried out research in TEA carbon dioxide, excimer and free-electron lasers at Heriot-Watt University in Edinburgh, Scotland and participated in ESA studies for a space based Doppler Lidar. Gary is responsible for the LAMP optics.

Zachary Warfield received a B.S. in mechanical engineering from University of Notre Dame in 1998 and a M.S. in Aeronautics & Astronautics from Massachusetts Institute of Technology in 2001. He currently is employed at the Jet Propulsion Laboratory, California Institute of Technology, in the Structures and Mechanisms Group of the Mechanical Engineering Section. He is currently the mechanical lead for the LAMP sensor development.

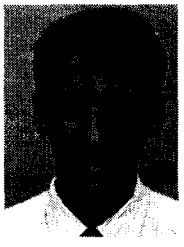

Dr. Malcolm Wright received the B.Sc. (hons) degree (1984) and M.Sc. degree (1986) in physics from Victoria University of Wellington, New Zealand, and Ph.D. degree (1992) in physics from the University of New Mexico, Albuquerque, NM with research undertaken for the latter at the Chemical Laser Branch of the Phillips Laboratory, Kirtland AFB, NM. Following postdoctoral research at the Center for High Technology Materials, University of New Mexico, he was with the Semiconductor Laser Branch of the Air Force Research Lab, Kirtland AFB, NM developing high power semiconductor lasers. Currently he is with the Optical Communications Group at the Jet Propulsion Lab., California Institute of Technology, developing laser based communication systems for future NASA flight projects. His research interests include dynamics of high speed lasers for free space optical communications and space qualification of semiconductor and fiber based lasers for space borne applications. He has authored numerous technical papers and presentations and is a member of the American Physical Society. Malcolm is responsible for the Pump and VCSEL lasers for LAMP